HHS Public Access

Author manuscript

Acta Biomater. Author manuscript; available in PMC 2016 February 01.

Published in final edited form as:

Acta Biomater. 2015 February ; 13: 61–67. doi:10.1016/j.actbio.2014.11.003.

Biphasic response of cell invasion to matrix stiffness in 3-dimensional biopolymer networks

Nadine R. Lang[†], **Kai Skodzek**[†], **Sebastian Hurst**[†], **Astrid Mainka**[†], **Julian Steinwachs**[†], **Julia Schneider**[†], **Katerina E. Aifantis**[‡], and **Ben Fabry**[†]

[†] Department of Physics, University of Erlangen- Nuremberg, Germany

[‡] Department of Civil Engineering and Engineering Mechanics, University of Arizona, Tucson, AR, USA

Abstract

When cells come in contact with an adhesive matrix, they begin to spread and migrate with a speed that depends on the stiffness of the extracellular matrix. On a flat surface, migration speed decreases with matrix stiffness mainly due to an increased stability of focal adhesions. In a 3-dimensional (3D) environment, cell migration is thought to be additionally impaired by the steric hindrance imposed by the surrounding matrix. For porous 3D biopolymer networks such as collagen gels, however, the effect of matrix stiffness on cell migration is difficult to separate from effects of matrix pore size and adhesive ligand density, and is therefore unknown. Here we used glutaraldehyde as a crosslinker to increase the stiffness of self-assembled collagen biopolymer networks independently of collagen concentration or pore size. Breast carcinoma cells were seeded onto the surface of 3D collagen gels, and the invasion depth was measured after 3 days of culture. Cell invasion in gels with pore sizes larger than 5 μm increased with higher gel stiffness, whereas invasion in gels with smaller pores decreased with higher gel stiffness. These data show that 3D cell invasion is enhanced by higher matrix stiffness, opposite to cell behavior in 2D, as long as the pore size does not fall below a critical value where it causes excessive steric hindrance. These findings may be important for optimizing the recellularization of soft tissue implants or for the design of 3D invasion models in cancer research.

INTRODUCTION

The ability of cells to migrate through their surrounding 3-dimensional (3D) extracellular matrix (ECM) is crucial for wound repair, immune responses, embryogenesis, tumor progression and metastasis formation, but also for the recellularization of biomaterials and the revascularization of porous implants [1-4]. Previous studies of cells grown on flat 2-dimensional (2D) substrates have shown that the mechanical properties - in particular the

Disclosure Statement

The authors declare no conflict of interest.

stiffness - of the underlying substrate influences cell migration [5, 6]. On a more rigid substrate, cells form more stable focal adhesions, which leads to a reduced migration speed and contributes to durotaxis where cells migrate in the direction of increasing substrate stiffness [7, 8]

In a 3D environment, the migrating cells must, in addition to adhesion forces, also overcome the resisting forces imposed by the surrounding matrix [9-11]. Resisting forces arise from steric effects as the cell moves through the matrix and deforms it. This steric hindrance depends on cell shape and cell mechanics but is also modulated by the effective mechanical properties of the matrix. For non-porous degradable PEG-based hydrogels, cell migration speed and migration persistence has been shown to decrease with increasing matrix stiffness [12]. In a porous matrix, however, the effective mechanical properties also depend on the porosity or the mesh size of the matrix [13-17].

3D cell migration studies where the matrix protein concentration and hence matrix stiffness was changed, however, have reported inconsistent data. Cell migration speed in a 3D porous collagen network was shown to decrease with increasing matrix protein concentration and hence higher stiffness [18]. By contrast, in a porous Matrigel network, cell migration speed was shown to exhibit a biphasic response, with a maximum speed at intermediate matrix protein concentrations [9]. These results are difficult to interpret, however, as matrix protein concentration not only determines the matrix stiffness but also pore size and adhesion ligand density [13, 14, 19], all of which can influence cell migration speed [9, 18, 20, 21].

In this study, we changed the pore size and stiffness of porous, fibrillar collagen gels independently, using the chemical crosslinker glutaraldehyde [22, 23]. The highly reactive aldehyde groups of glutaraldehyde bind covalently to the N- and C-terminal ends of the collagen fibrils and increase matrix stiffness without changing the pore size [24]. We show that a higher matrix stiffness promotes 3D cell invasion in gels with large pores where steric effects are small. By contrast, in gels with small pore sizes, an increasing matrix stiffness amplifies the steric hindrance of the matrix and therefore impairs cell invasion.

MATERIALS AND METHODS

Gel preparation

For collagen gels with a concentration of 2.4 mg/ml, we mixed 1.2 ml collagen G (4 mg/ml bovine collagen type I; Biochrome), 1.2 ml collagen R (2 mg/ml rat collagen type I; Serva, Heidelberg, Germany), 270 µl $NaHCO_3$ buffer (26.5mM) and 270 µl 10× DMEM (Biochrome), and adjusted to pH 10 with 43 µl 1M NaOH. All ingredients were kept on ice in order to prevent premature polymerization. For final collagen concentrations of 1.2 mg/ml, 0.6 mg/ml and 0.3 mg/ml, the solution was diluted with a mixture of 1 vol. part $NaHCO_3$ (26.5mM), 1 part 10× DMEM and 8 parts H_2O, adjusted to pH 10 with NaOH (1M). 1.2 ml of the final solution was pipetted in a 35 mm culture dish (Greiner, Germany), and gels were polymerized in a tissue culture incubator at 37°C, 5% CO_2 and 95% humidity for 2h. Afterwards, cell culture medium was added in order to prevent dehydration.

Crosslinking of collagen gels

Collagen gels were crosslinked for 1 h using 0.2% glutaraldehyde (25% stock solution, Merck, Darmstadt) in PBS (Invitrogen). After crosslinking, the gels were washed every 2 h with 2 ml of 20 mM TRIS buffer (Roth) for at least 12 times. Before adding cells, the gels were washed twice with cell culture medium.

Cell Culture

MDA-MB 231 cells were kept in 75cm^2 cell culture flasks with Dulbecco's modified Eagle's medium (DMEM 1g glucose, Greiner) and 10% fetal calf serum (FCS, Greiner) at 37°C, 5% CO_2 and 95% humidity. Cells were split every two days.

Invasion assay

50,000 cells were seeded on top of collagen gels and allowed to invade for 3 days at cell culture conditions. Afterwards, cells were fixed with 2ml of 2.5 % glutaraldehyde in PBS, and cell nuclei were stained with 1 μg/ml Hoechst 33342 (Sigma) for 20 minutes. To analyze the invasion profile, 3D image stacks with a z-distance of 2 μm were obtained with a motorized Leica 6000 inverse fluorescence microscope. The z-position of cell nuclei as a function of the invasion depth was determined in 36 fields of view using a custom-written Matlab script. The invasion profile was then computed as the cumulative probability to find a cell at or below a given depth. We defined a characteristic invasion depth as the invasion depth that was reached or exceeded by 5 % of the cells. This choice guarantees that we analyze only cells that have migrated away from the gel surface into the depth of the gel. Changes of invasion depth in response to changes in gel density and stiffness (see Fig. 3), however, remain qualitatively similar for lower or higher percentiles between 1% and 10%.

Magnetic tweezer microrheology

Stiffness measurements of collagen gels were performed with a magnetic tweezer setup as described in [25]. Fibronectin-coated 5μm superparamagnetic beads were bound on top of collagen gels for 1h. A staircase-like force step protocol was applied with 20 consecutive steps of 0.5 nN and 1 s duration, up to a maximum force of 10 nN. Bead displacements in response to force steps were measured with a microscope equipped with a CCD-camera (Orca ER, Hamamatsu) and a 20× 0.4 NA objective under bright field illumination. Bead displacements followed a weak power law at all force steps. The creep compliance was fitted to the equation [25, 26],

$$J(F,t) = J_0(F)\left(\frac{t}{t_0}\right)^{\beta(F)}$$

where $1/J_0(F)$ is the force-dependent differential creep modulus measured at t_0 = 1s, and $\beta(F)$ is the force-dependent power-law exponent.

Extensional rheometer

For measuring the stress-strain relationship of collagen under uniaxial stretch, a cylinder of collagen was cast between two parallel plates with holes arranged in a checkerboard pattern

(Fig 2c, inset). The plates were pretreated with Pluronic F-127 (Sigma-Aldrich,) to prevent adhesion of the gel. The lower plate was connected to a precision scale (AND GR-200), and the upper plate was mounted to a motorized micromanipulator (Eppendorf Injectman). The gel was vertically stretched at a rate of 10μm/s, and the weight change was continuously recorded. In this setup, the stretched gel has two different cross-sections between the plates and in the holes. This geometry corresponds to a serial connection of two mechanical elements with different cross-sections (A) and length (l_0). The Young's modulus E was calculated from the weight change ΔF and the change in total extension Δl as

$$E=\frac{\Delta F}{\Delta l}\left(\frac{l_{0,plates}}{A_{plates}}+2\frac{l_{0,holes}}{A_{holes}}\right)$$

The factor of 2 enters because there is an upper and a lower plate, both with the same hole geometry. The force-length relationship $\left(\frac{\Delta F}{\Delta l}\right)$ of the gel was corrected for the mechanical compliance of the device.

Pore size

The distribution of pore sizes in collagen gels were determined from confocal reflectance microscopy stacks as described in [19]. From binarized image stacks, the histogram of the nearest obstacle distance (Fig. 1e) was calculated and fitted to a Rayleigh distribution. The mean value of the Rayleigh distribution r_{mean} was corrected for missing fibers due to the blind spot effect in confocal reflectance microscopy [27]. For a 20× objective with NA=1.0, the cut-off angle above which fibers are invisible was determined to be θ_{cut}= 51°. r_{mean} was then converted into a more commonly used measure for the diameter of a pore as defined by the covering radius transform (CRT) [19, 28, 29]

$$d_{CRT}=2\times 1.82\times r_{mean}\times\sqrt{cos\,\theta_{cut}}$$

Note that in the following we report the pore diameter according to the CRT definition.

MMP inhibitor treatment

The broad-spectrum matrix metalloproteinase (MMP) inhibitor GM6001 (Merck Millipore) was used to block the activity of cell-secreted MMPs. 25mM GM6001in PBS were added directly after seeding the cells on top of the collagen gels.

Cell shape analysis

Cells were fixed with 4% paraformaldehyde (Thermo Fisher Scientific) in PBS for 20 min, stained with phalloidin TRITC (0.2 μg/ml, Sigma) for 1 h and then washed twice with PBS. Fluorescence image stacks (z-distance = 839.8 nm) of invaded cells were obtained with a confocal microscope (SP5X Leica upright microscope equipped with a 20× dip-in water immersion objective with NA=1.0). After a maximum intensity projection, the cell outline was determined with an edge detection algorithm implemented in Matlab and fitted to an ellipse. Cell eccentricity was computed as the ratio of the distance between the foci of the

ellipse and its major axis. Eccentricities close to 0 indicate circular shapes, while values close to 1 indicate highly elongated shapes.

Statistical analysis

All results are represented as arithmetic mean from at least three independent experiments ± one standard deviation or standard error of the mean, as indicated.

RESULTS

Morphological and mechanical properties of collagen networks

The pore size of reconstituted collagen networks have been shown to depend on the collagen monomer concentration and polymerization conditions including temperature and pH [13, 14, 17, 19, 30]. At the same time, the stiffness of these gels is expected to increase with higher collagen concentration [13, 31]. We polymerized collagen at monomer concentrations ranging from 0.3 mg/ml to 2.4 mg/ml at 37°C and pH 10, and confirmed that the resulting networks became denser with increasing collagen concentration (Fig. 1a-d). Quantification of confocal reflection microscopy image stacks using the nearest obstacle distance revealed a distribution of pore sizes that followed a Rayleigh distribution for all collagen concentrations measured (Fig. 1e). The average pore size decreased from 8.20 μm at the lowest collagen concentration to 2.92 μm at the highest concentration (Fig 1f). Repeating this experiment on different samples prepared on different days showed highly reproducible results (Fig. 1e inset black line, and Fig. 1f).

To measure the bulk stiffness (Young's modulus) of these gels in the linear regime, we applied a uniaxial strain and measured the resulting force with an extensional rheometer (Fig 2c, inset). The gel stiffness increased approximately linearly with increasing collagen concentrations from 45 Pa at the lowest concentration to 550 Pa at the highest concentration (Fig 2c).

To estimate the micromechanical properties of collagen at a force and deformation scale relevant for cells, we used a magnetic tweezer setup (Fig 2a inset). We applied forces between 1 nN and 10 nN to 5 μm diameter beads bound to the collagen gel surface, and measured the resulting bead displacements. Bead displacements were on the order of several micrometers except for 0.3 mg/ml collagen gels, where displacements exceeded 10 μm at the highest force (Fig 2a, black lines). All gels stiffened with increasing forces, with a more pronounced stiffening for higher concentrated gels (Fig 2b, black lines). Micromechanical stiffness scaled approximately linearly with collagen concentration similar to the bulk stiffness data.

Crosslinking with GA

Gel stiffness at the highest collagen concentration was below the stiffness reported for soft connective tissue such as brain tissue [32]. To increase the stiffness of reconstituted collagen gels without altering their morphology and pore size, we used the crosslinker glutaraldehyde [23]. Confocal imaging showed that the pore size was not affected by crosslinking (Fig. 1e inset and 1f, red lines and columns). Linear bulk stiffness measured with an extensional

rheometer was 6-fold higher compared to non-crosslinked gels (Fig. 2c). Microrheology measurements with magnetic beads also showed a pronounced stiffening of the crosslinked gels, with a stiffness that was approximately 4-fold higher compared to non-crosslinked gels (Fig. 2b). Gel displacements remained below 3 μm even at the highest forces (10 nN) and lowest collagen concentration (0.3 mg/ml) (Fig. 2a, red lines).

Cell invasion depends on mechanical and morphological properties

We next performed an invasion assay to evaluate the ability of tumor cells to migrate through gels with different stiffnesses and pore sizes. MDA-MB 231 breast carcinoma cells were seeded on top of the gels, and after three days of incubation, we determined the invasion profile as described in [33]. Cell invasiveness showed a pronounced biphasic response with collagen concentration: Invasion was poor for diluted gels (0.3 ml/ml), reached a maximum at a collagen concentration of 1.2 mg/ml, and then decreased at higher collagen concentrations (Fig 3a-e, black profiles and columns). When the collagen gels were stiffened with glutaraldehyde, a similar biphasic response was observed, but the maximum invasiveness shifted to lower collagen concentrations and larger pore sizes: Invasiveness greatly improved for the more diluted gels (0.3 and 0.6 mg/ml), started to decrease at intermediate concentrations (1.2 mg/ml) and stopped nearly completely at the highest gel density of 2.4 mg/ml (Fig 3a-e, red profiles and columns). Although the invasion behavior of MDA-MB 231 cells responded strongly to changes in matrix stiffness and pore size, the cell shape did not change and remained highly elongated, with eccentricities close to unity for all conditions (Fig 3 g-h).

Influence of matrix metalloproteinases on cell invasion

To investigate if cells rely on matrix degradation through secretion of metalloproteinases (MMPs) for invasion [34-36], we repeated the invasion assays in the presence of the broad-band MMP inhibitor GM 6001. Cell invasiveness in glutaraldehyde-stabilized gels was not altered by MMP-inhibition (Fig 3f, orange columns). This finding was expected as the glutaraldehyde-treated gels remain stable in the presence of MMPs (Fig. S1). Interestingly, MMP inhibition also had little or no effect in untreated gels (Fig 3f, grey columns), demonstrating that cell invasiveness in these cells did not depend critically on MMP secretion and matrix degradation. Only at the highest collagen concentration (2.4 mg/ml) did we find a reduced invasion in the presence of the MMP inhibitor.

DISCUSSION

In this study, we analyzed the invasive behavior of a breast carcinoma cell line in collagen gels of different stiffnesses, pore sizes and collagen concentrations. Cell invasiveness followed a biphasic response with a maximum invasiveness in gels at an intermediate collagen concentration, stiffness, and pore size. To evaluate the influence of stiffness changes without introducing changes in collagen concentration and pore size, we stiffened the gels by crosslinking with glutaraldehyde. Interestingly, gel stiffening lead to an increase of cell invasiveness in diluted gels with large pores, but to a decrease of cell invasiveness in dense gels with small pores. This resulted in a similar biphasic response as seen in the untreated gels but with a shift of the maximum invasiveness to larger pores (Fig 3e, f).

We confirmed that glutaraldehyde treatment did not alter the pore size, in line with previous data [24], which is an advantage over cross linking for example by non-enzymatic glycation where the pore sizes are affected [37]. A disadvantage of glutaraldehyde cross-linking, however, is the requirement to remove toxic unbound aldehyde groups from the gels by thorough washing with TRIS-Buffer over a time course of at least 24 h. Moreover, gels after glutaraldehyde treatment are considerably less susceptible to proteolytic degradation by cell-secreted matrix metalloproteinases, as shown by the stability of the reflection signal in confocal images recorded over the course of several hours in the presence 2 mg/ml of collagenase (Fig. S1). We therefore tested the effect of a broad-band metalloproteinase inhibitor on cell invasiveness both in native and in glutaraldehyde-treated collagen gels. We found no systematic influence of the metalloproteinase inhibitor on MDA-MB 231 cell invasiveness (Fig. 3e,f) and observed only a small effect in 2.4 mg/ml gels where cells have to migrate through a dense material, which indicates that MMP secretion is not essential for MDA-MB 231 invasion in our gels. Moreover, these data demonstrate that the effect of glutaraldehyde treatment on cell invasion was conferred mainly by stiffness changes of the matrix and not by inhibiting matrix degradation.

To characterize the Young's modulus of the collagen gels, we performed measurements with an extensional rheometer. As expected, collagen stiffness increased with increasing collagen concentration, in line with previous studies [13, 38, 39]. Here, we used a combination of rat and bovine collagen, which produces gels that are stiffer compared to gels polymerized from pure calf skin or rat tail collagen: Young's moduli of our gels are between 45 Pa (for 0.3 mg/ml gels) and 550 Pa (for 2.4 mg/ml gels), compared to pure calf skin collagen gels (1 -13 Pa for concentrations ranging from 0.5-1.5 mg/ml; [13]) or pure rat-tail collagen gels (5-60 Pa for concentrations ranging from 1-4 mg/ml) [31]. Thus, the stiffness of our gels before glutaraldehyde treatment is in the range of PEG-hydrogels (25-1200 Pa) [12] and ribose-crosslinked 1.5 mg/ml collagen gels (200-700 Pa) [37] that have been used for similar 3D cell migration studies. However, the stiffness of our gels is higher compared to that of Matrigel (8-50 Pa) [9].

After glutaraldehyde treatment, gel stiffness of our samples increased by 4-6 fold $_{\text{and}}$ reached values from 200 Pa to 3400 Pa, which is in the range of soft polyacrylamide gels used in numerous 2D traction studies, and of soft connective tissue [32]. To measure the mechanical behavior of collagen gels on a length scale more relevant for cells, we performed microrheology measurements with a magnetic tweezer. Bead displacements in response to a force step increased with time according to a weak power-law, with an exponent around 0.12 for control gels, suggesting a predominantly elastic behavior (Fig S2 a). After glutaraldehyde treatment, the power-law exponent decrease to values below 0.05 (Fig S2 b), indicating that crosslinked gels are nearly perfectly elastic, in agreement with previous findings [40]. Micromechanical gel stiffness roughly scaled with the bulk stiffness for the different collagen concentrations, although the increase of the microscale stiffness after glutaraldehyde treatment was somewhat less pronounced (2-4-fold) compared to the bulk stiffness. This can be explained by the higher mechanical stress levels in the magnetic tweezer experiments that lead to a gel stiffening (Fig. 2b) and, as shown previously, to a collapse of the differential force-displacement responses for different gels [40].

From the magnetic bead measurements where we apply forces between 0.5-10 nN, we estimate that the traction force of a single focal adhesion site, which has been evaluated to be around 5 nN/μm^2 [41], cannot deform a dense collagen network by more than a few microns, and even less than 1 μm in the case of glutaraldehyde-treated gels. This is in agreement with previous results of a reduced translocation of fibers by cells seeded in dense collagen gels [31]. Given that dense gels of 2.4 mg/ml have a pore size below 3 μm, the decreased cell invasiveness at high collagen concentrations in particular after glutaraldehyde treatment can thus be explained by a strong steric hindrance of the collagen fiber network. Inhibition of matrix metalloproteinases had only minor effects on the invasion behavior of breast carcinoma cells studied here. Our data show that the combination of a small pore sizes with a high gel stiffness can severely impair cell invasion.

It is less clear why cell invasiveness was also impaired in soft diluted gels with large pore sizes but was increased after glutaraldehyde treatment (Fig. 3e). Our data of reduced 3D invasion in soft gels is in agreement with recent data showing that the migration speed of cells in compliant microfabricated channels decreased with decreasing matrix stiffness, mostly due to poor cell polarization [42]. The microfabricated channels with diameters between 10 - 40 μm, however, were as large or larger than the cell diameter, and thus steric hindrance did not play a role in that study. In fact, according to another recent study where cells migrated through porous but stiff membranes of a Boyden chamber, steric hindrance effects emerge only for channel diameters below 5 μm, with some cell lines being able to migrate through pores with diameters below 1 μm [18].

On the one hand, our observation of impaired 3D invasion in soft gels is in contrast to reports that cells tend to migrate faster on soft planar 2D substrates [5, 7, 43]. On the other hand, our data are in line with more recent studies that showed a biphasic response of 2D cell migration speed to substrate stiffness; cells on soft substrates failed to polarize and therefore did no migrate persistently [42, 44]. However, we see a high degree of cell elongation even in untreated dilute gels with low stiffnesses in the range of 50 -100 Pa (Fig. 3g-h). Therefore, the impaired invasion in the softest gels was not attributable to impaired cell polarization but may be a sign of cellular mechanotransduction. According to a model for adhesion-independent cell migration [45], channel-like confinements lead to an increase of cell internal hydrostatic pressure, which in turn - by some unknown mechanism - enhances actin polymerization and thus cell protrusions and cell movements. Although cell migration and invasion in collagen networks is adhesion-dependent [46], it is plausible that cell internal pressure and actin turnover dynamics may also increases as cells squeeze through narrow pores. We have not tested this hypothesis in our study, but it is consistent with our observation that cell invasion decreases in diluted and soft gels. Finally, it is also possible that cells in soft gels may become durotactically trapped in regions with a higher local stiffness.

Conclusion

Our study demonstrates the critical role of matrix stiffness for cell migration and invasiveness in a porous 3D biopolymer network such as a collagen gel. Cells fail to invade very soft matrices, whereas high matrix stiffness promotes 3D cell invasion as long as the

pore size remains above a critical value. These findings may be important for optimizing the re-cellularization of soft tissue implants or for the design of 3D invasion models in cancer research.

Supplementary Material

Refer to Web version on PubMed Central for supplementary material.

Acknowledgements

This work was supported by grants from the Deutsche Forschungsgemeinschaft, the Emerging Fields Initiative of the University of Erlangen-Nuremberg, the National Institutes of Health, and the European Research Council.

REFERENCES

1. Friedl P, Wolf K. Proteolytic interstitial cell migration: a five-step process. Cancer Metastasis Rev. 2009
2. Friedl P, Gilmour D. Collective cell migration in morphogenesis, regeneration and cancer. Nat Rev Mol Cell Biol. 2009; 10:445–57. [PubMed: 19546857]
3. Martin P, Parkhurst SM. Parallels between tissue repair and embryo morphogenesis. Development. 2004; 131:3021–34. [PubMed: 15197160]
4. Lecaudey V, Gilmour D. Organizing moving groups during morphogenesis. Curr Opin Cell Biol. 2006; 18:102–7. [PubMed: 16352429]
5. Pelham RJ Jr. Wang Y. Cell locomotion and focal adhesions are regulated by substrate flexibility. Proc Natl Acad Sci U S A. 1997; 94:13661–5. [PubMed: 9391082]
6. Lautscham LA, Lin CY, Auernheimer V, Naumann CA, Goldmann WH, Fabry B. Biomembrane-mimicking lipid bilayer system as a mechanically tunable cell substrate. Biomaterials. 2014; 35:3198–207. [PubMed: 24439398]
7. Lo CM, Wang HB, Dembo M, Wang YL. Cell movement is guided by the rigidity of the substrate. Biophys J. 2000; 79:144–52. [PubMed: 10866943]
8. Wang HB, Dembo M, Hanks SK, Wang Y. Focal adhesion kinase is involved in mechanosensing during fibroblast migration. Proc Natl Acad Sci U S A. 2001; 98:11295–300. [PubMed: 11572981]
9. Zaman MH, Trapani LM, Siemeski A, Mackellar D, Gong H, Kamm RD, et al. Migration of tumor cells in 3D matrices is governed by matrix stiffness along with cell-matrix adhesion and proteolysis. Proc Natl Acad Sci U S A. 2006; 103:10889–94. [PubMed: 16832052]
10. Doyle AD, Wang FW, Matsumoto K, Yamada KM. One-dimensional topography underlies three-dimensional fibrillar cell migration. J Cell Biol. 2009; 184:481–90. [PubMed: 19221195]
11. Friedl P, Brocker EB. The biology of cell locomotion within three-dimensional extracellular matrix. Cell Mol Life Sci. 2000; 57:41–64. [PubMed: 10949580]
12. Ehrbar M, Sala A, Lienemann P, Ranga A, Mosiewicz K, Bittermann A, et al. Elucidating the Role of Matrix Stiffness in 3D Cell Migration and Remodeling. Biophys J. 2011; 100:284–93. [PubMed: 21244824]
13. Yang YL, Kaufman LJ. Rheology and confocal reflectance microscopy as probes of mechanical properties and structure during collagen and collagen/hyaluronan self-assembly. Biophys J. 2009; 96:1566–85. [PubMed: 19217873]
14. Yang YL, Motte S, Kaufman LJ. Pore size variable type I collagen gels and their interaction with glioma cells. Biomaterials. 2010; 31:5678–88. [PubMed: 20430434]
15. Raub CB, Putnam AJ, Tromberg BJ, George SC. Predicting bulk mechanical properties of cellularized collagen gels using multiphoton microscopy. Acta biomaterialia. 2010; 6:4657–65. [PubMed: 20620246]
16. Piechocka IK, Bacabac RG, Potters M, Mackintosh FC, Koenderink GH. Structural hierarchy governs fibrin gel mechanics. Biophys J. 2010; 98:2281–9. [PubMed: 20483337]

17. Wood GC, Keech MK. The formation of fibrils from collagen solutions. 1. The effect of experimental conditions: kinetic and electron-microscope studies. Biochem J. 1960; 75:588–98. [PubMed: 13845809]
18. Wolf K, Te Lindert M, Krause M, Alexander S, Te Riet J, Willis AL, et al. Physical limits of cell migration: Control by ECM space and nuclear deformation and tuning by proteolysis and traction force. J Cell Biol. 2013; 201:1069–84. [PubMed: 23798731]
19. Lang NR, Muenster S, Metzner C, Krauss K, Schuermann S, Lange J, et al. Estimating the 3D pore size distribution of biopolymer networks from directionally biased data. Biophys J. 2013; 105:1967–75. [PubMed: 24209841]
20. DiMilla PA, Stone JA, Quinn JA, Albelda SM, Lauffenburger DA. Maximal migration of human smooth muscle cells on fibronectin and type IV collagen occurs at an intermediate attachment strength. J Cell Biol. 1993; 122:729–37. [PubMed: 8335696]
21. Engler A, Bacakova L, Newman C, Hategan A, Griffin M, Discher D. Substrate compliance versus ligand density in cell on gel responses. Biophys J. 2004; 86:617–28. [PubMed: 14695306]
22. Bowes JH, Cater CW. The interaction of aldehydes with collagen. Biochim Biophys Acta. 1968; 168:341–52. [PubMed: 5748675]
23. Migneault I, Dartiguenave C, Bertrand MJ, Waldron KC. Glutaraldehyde: behavior in aqueous solution, reaction with proteins, and application to enzyme crosslinking. Biotechniques. 2004; 37:790–6, 8-802. [PubMed: 15560135]
24. Vader D, Kabla A, Weitz D, Mahadevan L. Strain-induced alignment in collagen gels. PLoS One. 2009; 4:e5902. [PubMed: 19529768]
25. Kollmannsberger P, Fabry B. High-Force Magnetic Tweezers with Force Feedback for Biological Applications. Rev Sci Instrum. 2007; 78:114301–1-6. [PubMed: 18052492]
26. Kollmannsberger P, Fabry B. Linear and Nonlinear Rheology of Living Cells. Annu Rev Mater Res. 2011; 41:75–97.
27. Jawerth LM, Münster S, Vader DA, Fabry B, Weitz DA. A Blind Spot in Confocal Reflection Microscopy: The Dependence of Fiber Brightness on Fiber Orientation in Imaging Biopolymer Networks. Biophys J. 2009; 98:L01–L3.
28. Mickel W, Muenster S, Jawerth LM, Vader DA, Weitz DA, Sheppard AP, et al. Robust Pore Size Analysis of Filamentous Networks From 3D Confocal Microscopy. Biophys J. 2008; 95:6072–80. [PubMed: 18835899]
29. Munster S, Fabry B. A simplified implementation of the bubble analysis of biopolymer network pores. Biophys J. 2013; 104:2774–5. [PubMed: 23790386]
30. Yang YL, Leone LM, Kaufman LJ. Elastic moduli of collagen gels can be predicted from two-dimensional confocal microscopy. Biophys J. 2009; 97:2051–60. [PubMed: 19804737]
31. Miron-Mendoza M, Seemann J, Grinnell F. The differential regulation of cell motile activity through matrix stiffness and porosity in three dimensional collagen matrices. Biomaterials. 2010; 31:6425–35. [PubMed: 20537378]
32. Discher DE, Janmey P, Wang YL. Tissue cells feel and respond to the stiffness of their substrate. Science. 2005; 310:1139–43. [PubMed: 16293750]
33. Koch TM, Muenster S, Bonakdar N, Buttler JP, Fabry B. 3D Traction Forces in Cancer Cell Invasion. PloS One. 2012; 7:e33476. [PubMed: 22479403]
34. Sabeh F, Ota I, Holmbeck K, Birkedal-Hansen H, Soloway P, Balbin M, et al. Tumor cell traffic through the extracellular matrix is controlled by the membrane-anchored collagenase MT1-MMP. J Cell Biol. 2004; 167:769–81. [PubMed: 15557125]
35. Rowe RG, Weiss SJ. Navigating ECM barriers at the invasive front: the cancer cell-stroma interface. Annu Rev Cell Dev Biol. 2009; 25:567–95. [PubMed: 19575644]
36. Wolf K, Friedl P. Extracellular matrix determinants of proteolytic and non-proteolytic cell migration. Trends Cell Biol. 2011; 21:736–44. [PubMed: 22036198]
37. Mason BN, Starchenko A, Williams RM, Bonassar LJ, Reinhart-King CA. Tuning three-dimensional collagen matrix stiffness independently of collagen concentration modulates endothelial cell behavior. Acta biomaterialia. 2013; 9:4635–44. [PubMed: 22902816]
38. Lindstrom SB, Kulachenko A, Jawerth L, Vader DA. Finite strain, finite-size mechanics of rigidly cross-linked biopolymer networks. Soft Matter. 2013 DOI:10.1039/C3SM50451D.

39. Stein AM, Vader DA, Weitz DA, Sander LM. The Micromechanics of Three-Dimensional Collagen-I Gels. Complexity. 2010 DOI 10.1002/cplx.20332.

40. Munster S, Jawerth LM, Leslie BA, Weitz JI, Fabry B, Weitz DA. Strain history dependence of the nonlinear stress response of fibrin and collagen networks. Proc Natl Acad Sci U S A. 2013; 110:12197–202. [PubMed: 23754380]

41. Balaban NQ, Schwarz US, Riveline D, Goichberg P, Tzur G, Sabanay I, et al. Force and focal adhesion assembly: a close relationship studied using elastic micropatterned substrates. Nat Cell Biol. 2001; 3:466–72. [PubMed: 11331874]

42. Pathak A, Kumar S. Independent regulation of tumor cell migration by matrix stiffness and confinement. Proc Natl Acad Sci U S A. 2012; 109:10334–9. [PubMed: 22689955]

43. Pelham RJ Jr. Wang YL. Cell locomotion and focal adhesions are regulated by the mechanical properties of the substrate. Biol Bull. 1998; 194:348–9. discussion 9-50. [PubMed: 11536880]

44. Peyton SR, Putnam AJ. Extracellular matrix rigidity governs smooth muscle cell motility in a biphasic fashion. J Cell Physiol. 2005; 204:198–209. [PubMed: 15669099]

45. Hawkins RJ, Piel M, Faure-Andre G, Lennon-Dumenil AM, Joanny JF, Prost J, et al. Pushing off the walls: a mechanism of cell motility in confinement. Phys Rev Lett. 2009; 102:058103. [PubMed: 19257561]

46. Mierke CT, Frey B, Fellner M, Herrmann M, Fabry B. Integrin {alpha}5{beta}1 facilitates cancer cell invasion through enhanced contractile forces. J Cell Sci. 2010; 124:369–83. [PubMed: 21224397]

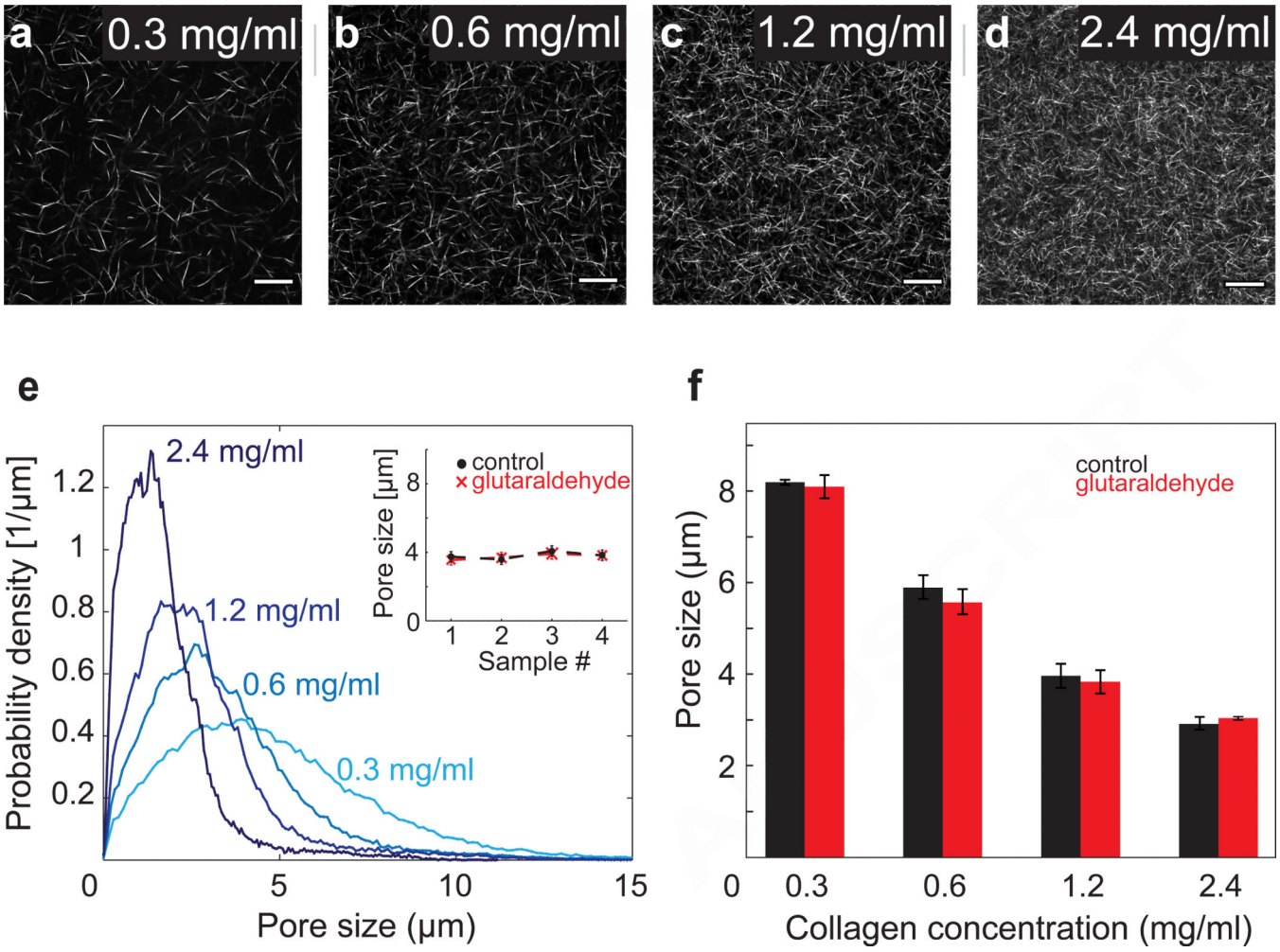

FIGURE 1.

Morphological properties of collagen networks. (**a-d**) Optical section (total thickness 0.350 µm) of collagen gels with concentrations 0.3mg/ml (a), 0.6mg/ml (b), 1.2 mg/ml (c) and 2.4 mg/ml (d) imaged with confocal reflection microscopy. Scale bar is 20µm. (**e**) Pore size distributions from the same data sets as in (a-d) followed a Rayleigh–distribution. With increasing collagen monomer concentration, the pore sizes became smaller. Inset: Characteristic pore size of a 1.2 mg/ml collagen gel (mean ± sd from 5 fields of view of 4 gels for each condition). Glutaraldehyde treatment did not change the pore size of the gels. (**f**) Pore sizes versus collagen concentration (mean ± sd, from 5 fields of view of at least 3 gels for each condition).

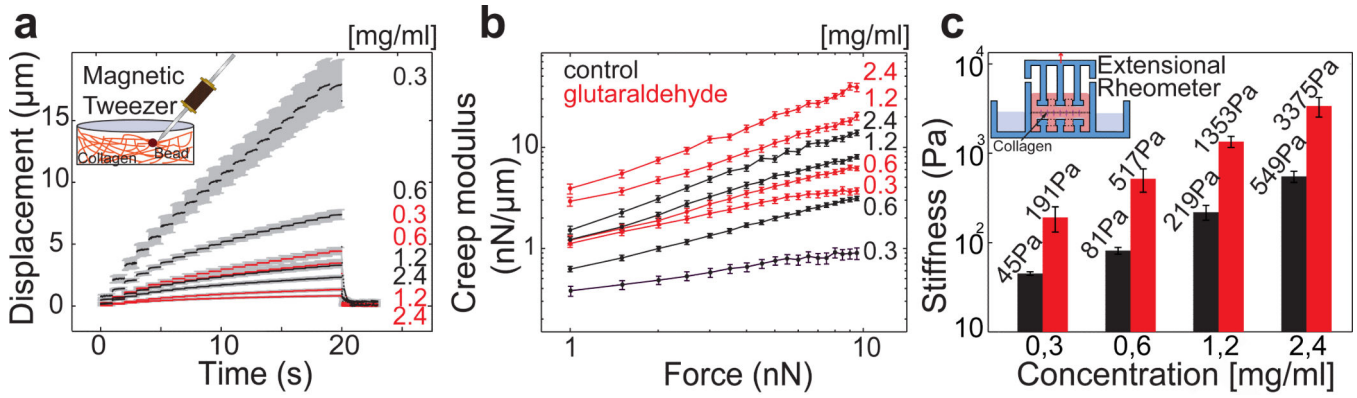

FIGURE 2.

Mechanical properties of collagen networks. (**a**) Bead displacement in response to a staircase-like force protocol (from 0.5 nN with 0.5 nN increments every second) applied using magnetic tweezers. With increasing collagen monomer concentration and after glutaraldehyde treatment (red), bead displacements for a given force decreased. Error bars indicate SE around the mean of at least 30 beads per condition measured on at least 3 different gel samples. Inset: magnetic tweezer setup (**b**) Microrheological creep modulus versus applied force calculated from the data shown in Fig. 2a. The creep modulus increased with increasing monomer concentration and after glutaraldehyde treatment (red). (**c**) Stiffness (Young's modulus) from control gels (black) and gels treated with glutaraldehyde (red) measured with an extensional rheometer (inset) (mean ± se of at least 3 different gel samples).

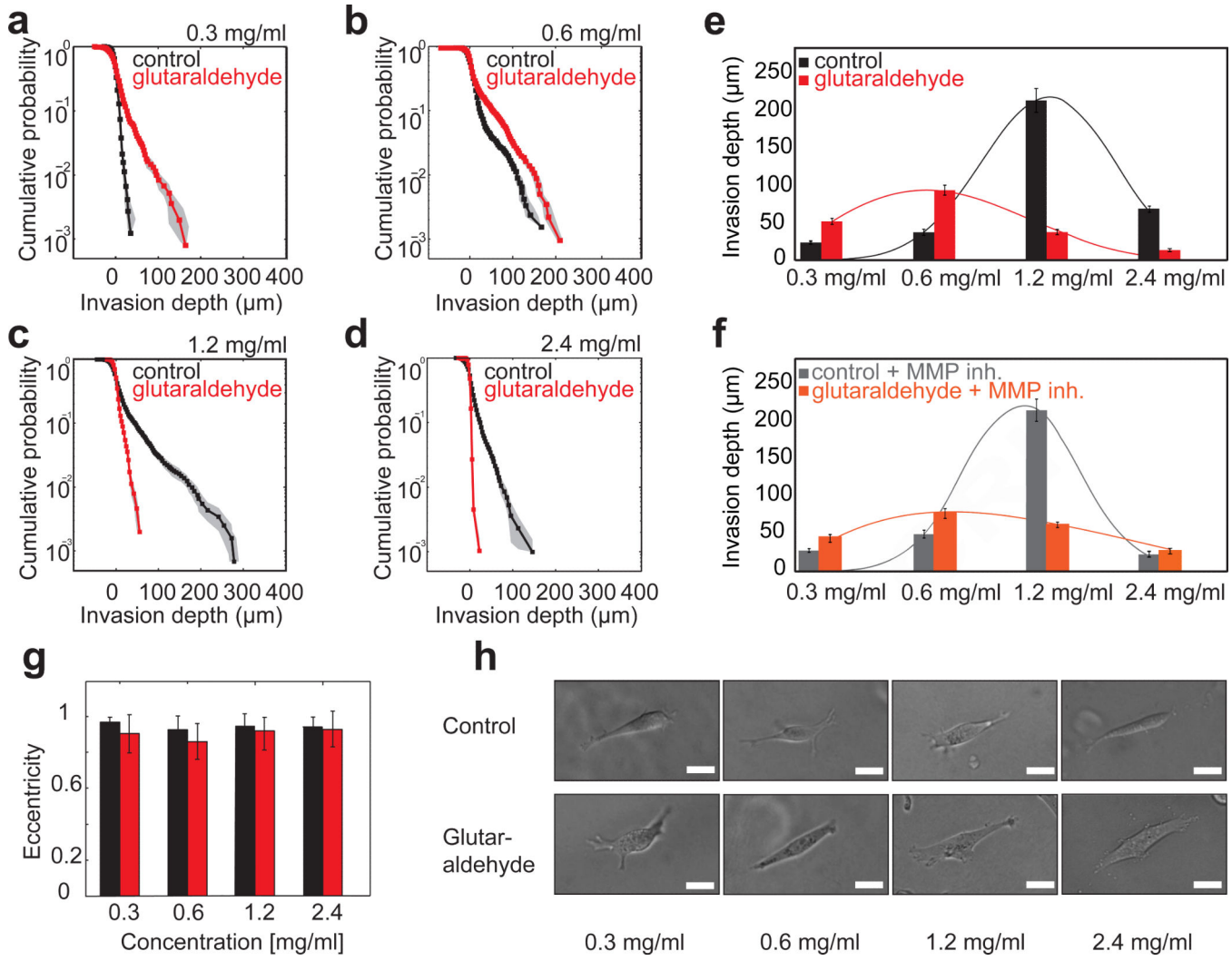

FIGURE 3.

Cell invasion depends on matrix pore size and stiffness. (**a-d**) The invasion profile of MDA-MB 231 cells is expressed as the probability to find a cell at or below a given invasion depth in control gels (black) and glutaraldehyde-treated gels (red). Shaded areas indicate ±1 SE around the mean from at least 90 fields of view measured on at least 3 different gels prepared on different days. (**e,f**) From the invasion profiles, a characteristic invasion depth was defined as the depth that 5% of the cells reached within 3 days of culture. As a guide to the eye, a log-normal curve was fitted to the results. (**e**) Cell invasion showed a biphasic dependence on collagen concentration, with a maximum around 1.2 mg/mg (black bars). This maximum was shifted towards smaller collagen concentrations around 0.6 mg/mg in glutaraldehyde-treated gels (red bars). (**f**) A similar biphasic response of cell invasiveness was observed after cell treatment with the MMP-inhibitor GM6001 (25 mM). (**g**) Bright-field images of invaded cells showed elongated shapes for all conditions. Scale bar is 20 μm. (**h**) The eccentricity of invaded cells (mean ± SE of at least 20 cells) did not change with collagen concentration or glutaraldehyde treatment (red bars).